

Supporting Information

Force Triggered Self-destructive Hydrogels

Tharindu Rajasooriya, Hiroaki Ogasawara, Yixiao Dong, Joseph Nicholas Mancuso, and Khalid Salaita

Table 1: Sequence of DNA/RNA used in this study.

Name	Sequence (5' to 3')
Locked HP for PAGE	TAC CGC ACA GAT GCG TTA TTT TAT TTT ATT TTTT AAT AAA ATA AAA TAA AAG AGC GCC ACG TAG
Locking strand for locked HP	CTA CGT GGC GCT CTT CGC ATC TGT GCG GTA
DNA HP (80% GC content)	GG CCC GAC GTG CGA CCG GCG TCG CAC GTC GGG CC
dsDNA sequence 1	GCC GCC CGG CGG GCC GGG CGC CGG CCC GCG
dsDNA sequence 2	CGC GGG CCG GCG CCC GGC CCG CCG GGC GGC
ssDNA	CT GTC CTG ACG TGC TTC GTC CTG ACG TGC GGC TC
DNA HP with PEG ₆ Spacer	GG CCT GAC GTG CGG C/iSp18/G CCG CAC GTC AGG CC
DNA HP with (PEG ₆) ₂ Spacer	GG CCT GAC GTG CGG C/iSp18//iSp18/G CCG CAC GTC AGG CC
PS DNA HP with PEG ₆ Spacer	GG CCT GAC GTG CGG C*/iSp18/*G CCG CAC GTC AGG CC
PS DNA HP with (PEG ₆) ₂ Spacer	GG CCT GAC GTG CGG C*/iSp18/*iSp18/*G CCG CAC GTC AGG CC
PS ssDNA	CTG TCC TGA CGT GCT* /iSp18/*CC TGA CGT GCG GCT C
Bisamine modified PS ssDNA	/5AmMC6/ CTG TCC TGA CGT GCT* /iSp18/*CC TGA CGT GCG GCT C /3AmMO/
Bisamine modified 80% GC HP Spacer	/5AmMC6/GG CCT GAC GTG CGG C*/iSp18/*G CCG CAC GTC AGG CC/3AmMO/
Bisamine modified 100% GC HP	/5AmMC6/GGC CCG CCG GGC GGC* /iSp18/*GCC GCC CGG CGG GCC /3AmMO/

Bisamine modified 0% GC HP	/5AmMC6/TAT ATA ATT AAT ATT */iSp18/* AAT ATT AAT TAT ATA /3AmMO/
Activator DNA targeted sequence ^[1]	TTT AAT TTT GTT AAA GAA GAT GGT ATG TGG AAG TTA GAT T
Activator DNA non targeted sequence ^[1]	AAT CTA ACT TCC ACA TAC CAT CTT CTT TAA CAA AAT TAA A
gRNA for Cas12a ^[1]	GGG UAA UUU CUA CUA AGU GUA GAU UUA AAG AAG AUG GUA UGU GG

* Indicates the phosphorothioate (PS) modification

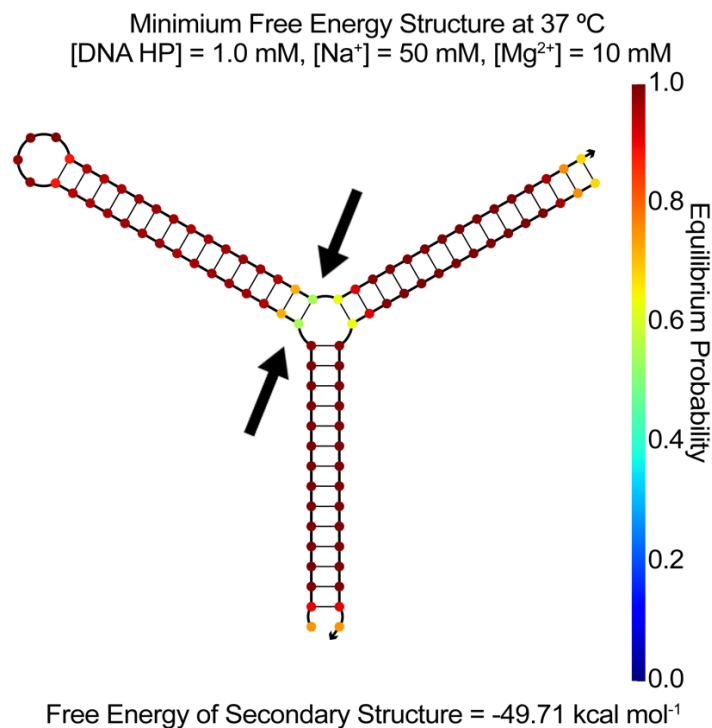


Figure S1: Minimum free energy structure for the DNA HP with the locking strand, obtained using the NUPACK online DNA simulator.^[2] The identified base pairs with the arrows (green color) show lower probability (~50%) of base pairing. These positions might be vulnerable for CRISPR cas12a activity, boosting the cleavage of the probe.

Time (hours)				24	12	6	3	2	1
Guide RNA (gRNA)	+	-	-	+	+	+	+	+	+
Activator DNA (targeted sequence)	-	+	-	+	+	+	+	+	+
Activator DNA (non-targeted sequence)	-	+	-	+	+	+	+	+	+
DNA hairpin	-	-	+	+	+	+	+	+	+
Cas12a	-	-	-	+	+	+	+	+	+

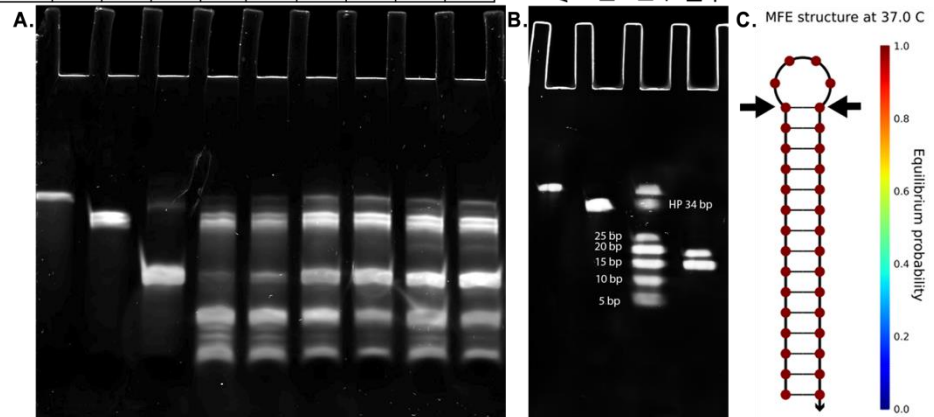


Figure S2: Stability of the DNA HP under the activated Cas12a activity. **(A)** Denaturing PAGE analysis of the Cas12a-cleaved DNA HPs reacted over different time points. Increasing the incubation time showed decreasing the area for the DNA HP due to Cas12a activity. **(B)** Denaturing PAGE analysis of Cas12a cleaved DNA HPs with the DNA ladder. **(C)** Predicted structure of the DNA HP using NUPACK online oligo simulator software. The two arrows indicating base pairs that could be vulnerable to the Cas12a activity according to the PAGE data.

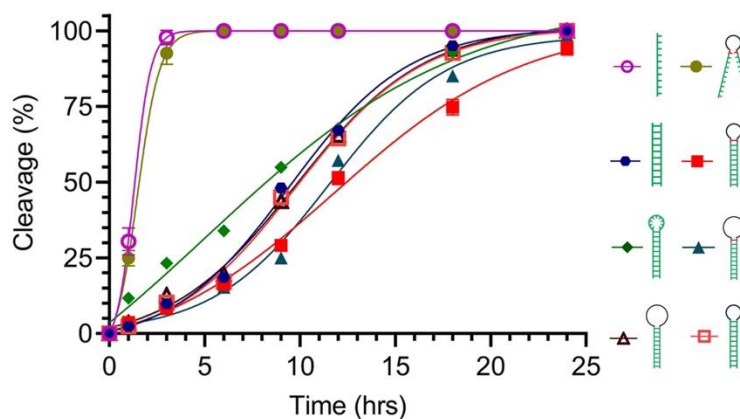


Figure S3: Plot of the time-dependent Cas12a cleavage of eight DNA structures in 1X NEB r2.1 buffer at room temperature evaluated by HPLC analysis. The two ssDNA crosslinkers exhibit the fastest Cas12a-mediated hydrolysis. DNA duplex with PS

modification at the junction with the PEG loop (PEG₆ and (PEG₆)₂) showed the highest resistance to Cas12a activity.

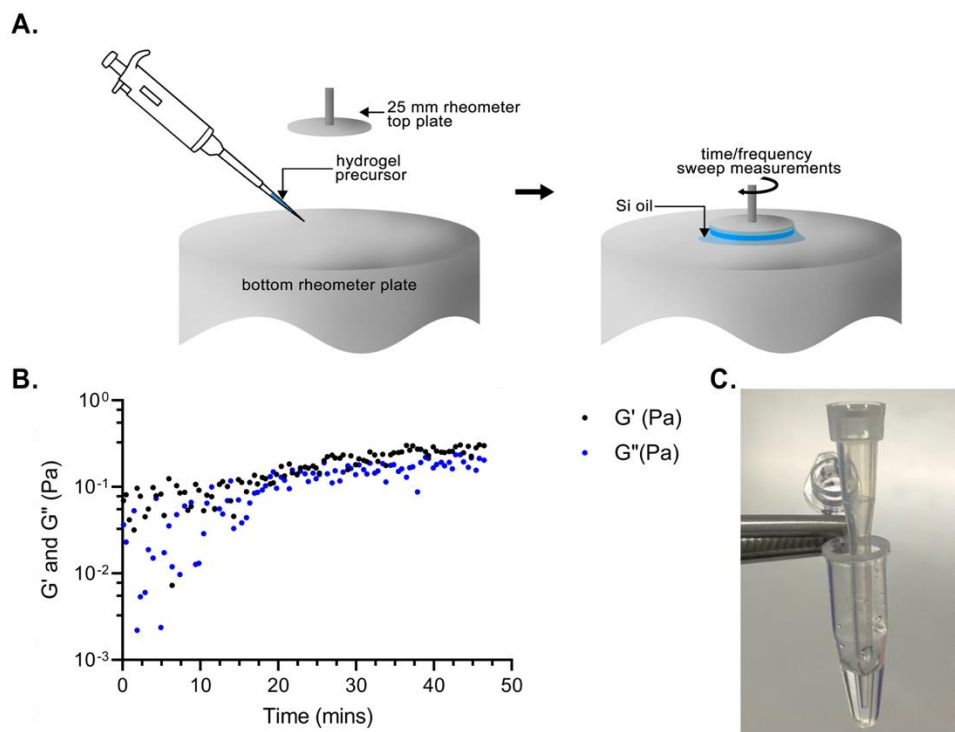


Figure S4: Confirmation that the tPEG-NHS (Mw: 10k)-bisamine DNA hydrogel does not gelate. **(A)** Experimental setup for time sweep and frequency sweep experiments **(B)** Representative plot of time-dependent measurement of storage modulus (G') and loss modulus (G'') of the DNA crosslinked hydrogel synthesized by NHS-amine reaction. Time sweep experiment showed no distinguishable crossover point between G' and G'' , suggesting failure of hydrogel formation. **(C)** Photograph of the DNA crosslinked hydrogel synthesized by NHS-amine reaction. After incubation of the precursors (tPEG-NHS (Mw: 10k) = 3.0 mM and diamine DNA (HPLC purified) = 6.0 mM) at 1x KPi buffer (pH = 8.4) and 37 °C for 30 minutes, a 10 μ L tip was added to confirm the lack of gel formation. The tip was immediately sank to the bottom of the PCR tube confirming the failure of hydrogel formation.

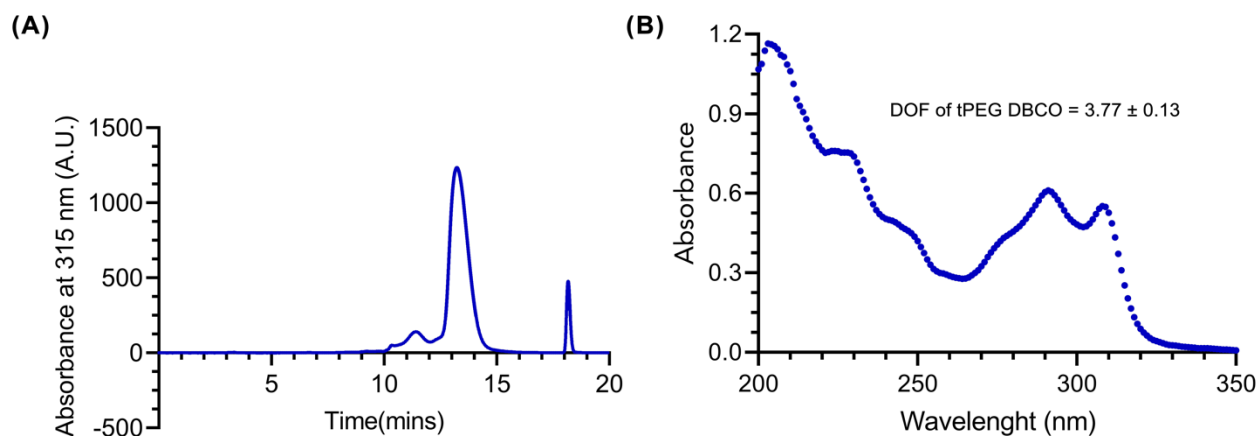


Figure S5: Characterization of synthesis of tPEG-DBCO ($M_w = 10\text{k g mol}^{-1}$) **(A)** Reverse phase HPLC chromatogram of the synthesized tPEG-DBCO. The chromatogram peak at 13.5 minutes was identified as tPEG-DBCO. **(B)** UV-Vis spectra of the synthesized tPEG DBCO. The characteristic peaks at 290 nm and 307 nm were observed and the data was consistent with the previous work done by Barker et al. and Webber et al.^[3] The determined molar absorption coefficient was used to determine degree of functionalization (DOF).

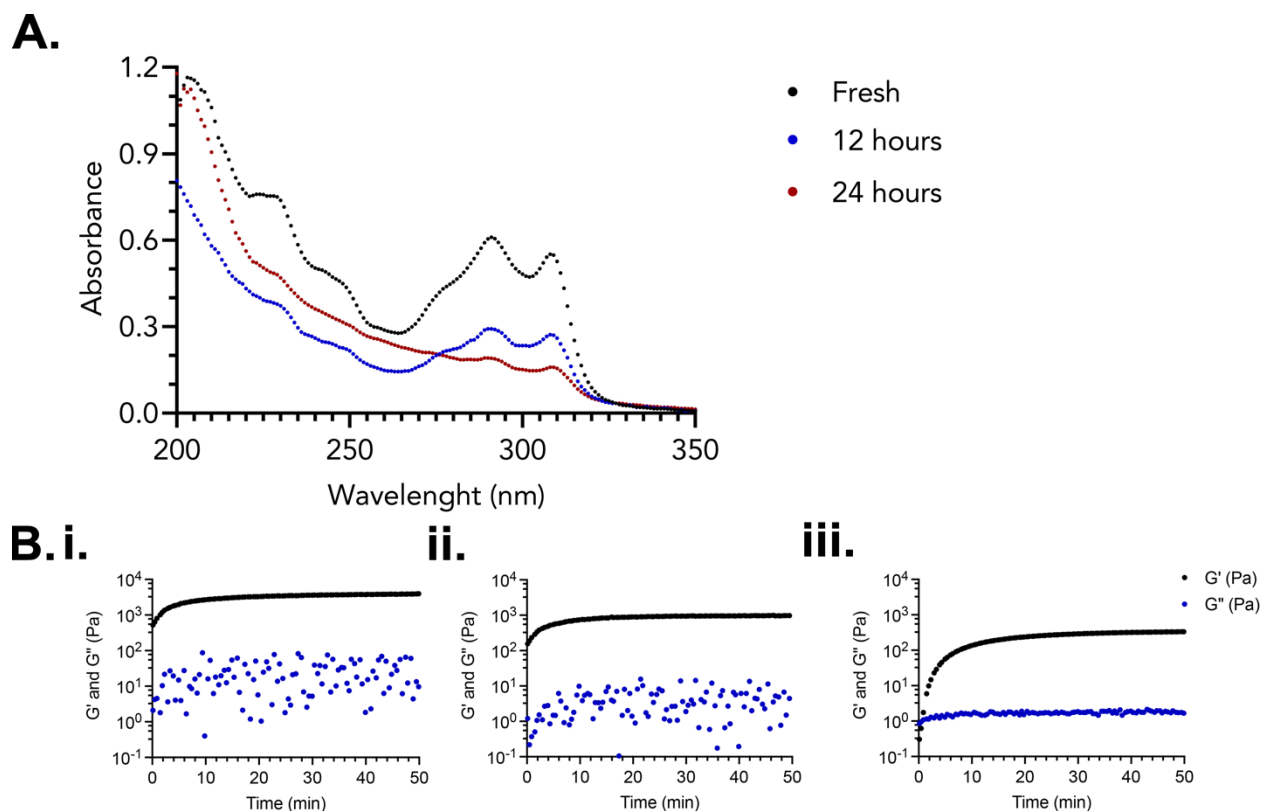


Figure S6: Characterization of the degradation of tPEG-DBCO over time. **(A)** The plot of UV-Vis spectra of tPEG-DBCO after incubation in aqueous media at different time points. The freshly prepared solution left at room temperature for 12 hrs and 24 hrs show significant decrease in the absorbance at 290 nm and 307 nm peaks due to DBCO degradation. All the samples used in the experiment had equal concentrations at $t=0$. **(B)** Representative plot of time-dependent measurement of G' and G'' of the hydrogels by crosslinking fresh and degraded tPEG-DBCO ($M_w = 10\text{ k g mol}^{-1}$) and tPEG-azide ($M_w = 10\text{ k g mol}^{-1}$). **(i)** Using freshly synthesized tPEG-DBCO ($G'_{\text{max}} = 3972$ Pa at $t = 50$ min) **(ii)** Using tPEG-DBCO solution left at room temperature for 12 hrs ($G'_{\text{max}} = 972$ Pa $t = 50$ min) **(iii)** Using tPEG-DBCO solution left at room temperature for 24 hrs ($G'_{\text{max}} = 334$ Pa $t = 50$ min).

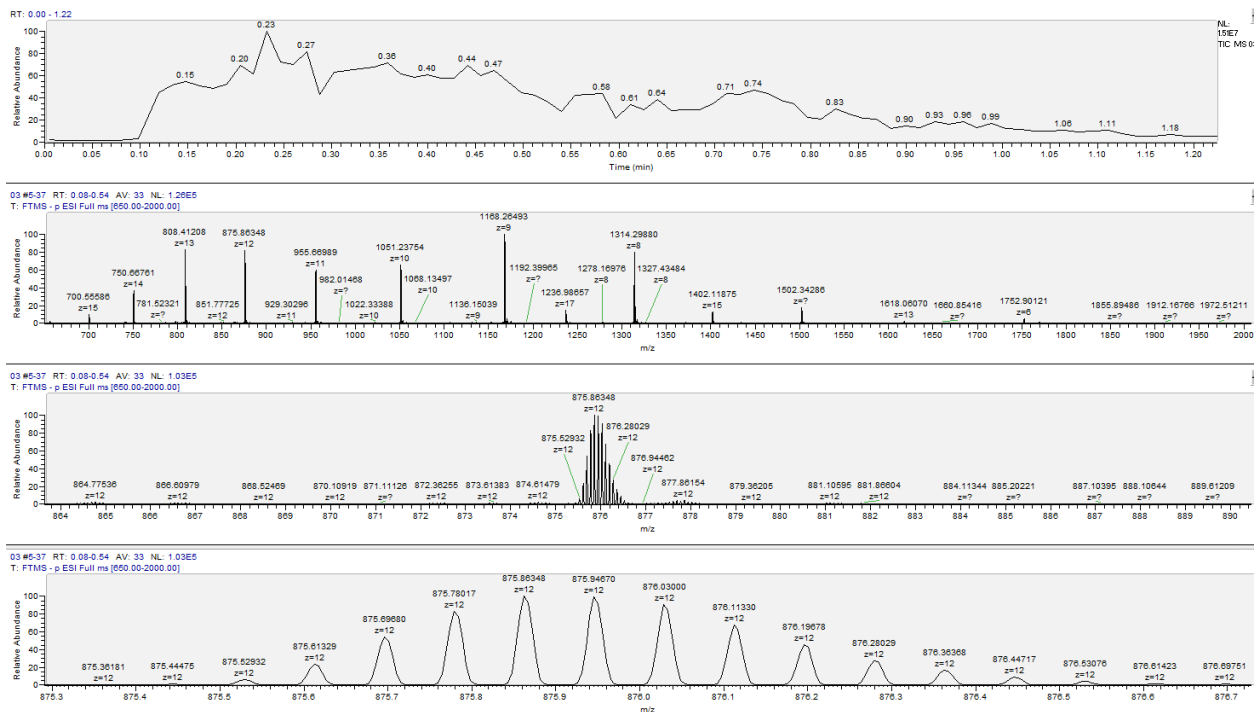


Figure S7: Observed ESI mass spectra for the bis azide-modified DNA HP. Deconvoluted molecular weight from the spectra was $10522.4 \text{ g mol}^{-1}$. The expected molecular weight was $10524.3 \text{ g mol}^{-1}$.

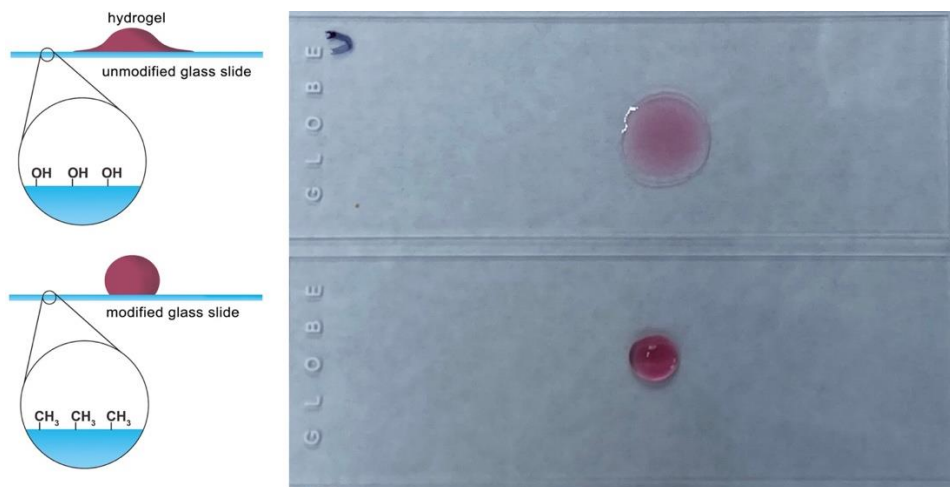


Figure S8: Photograph of the hydrogel to show importance of the use of hydrophobic glass slides. **(top)**. The glass slide without dimethyldichlorosilane modification. The precursor solution spreads with a greater surface area, resulting in smaller hydrogel thickness. **(bottom)**. The glass slide with hydrophobic dimethyldichlorosilane

modification. Due to the hydrophobic modification of glass slides, the hydrogel formed a more thick pebble-like structure.

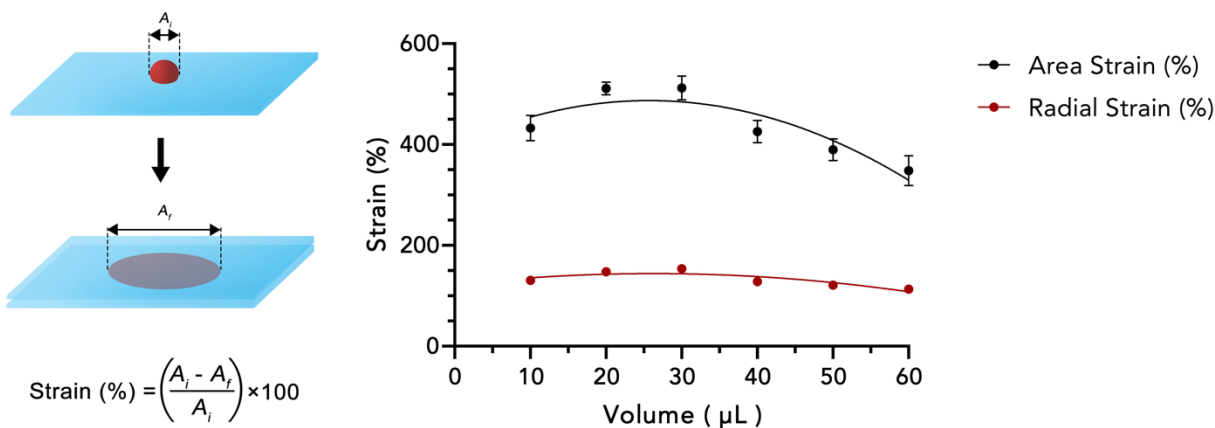


Figure S9: Plot of the radial and area strain when different volumes (V) of hydrogels were used, but the spacer gap was kept constant ($200 \mu\text{m}$). The area strain was measured using ImageJ and the radial strains were calculated by using the initial area measurements from the ImageJ. The maximum strain was observed at $V = 30 \mu\text{L}$.

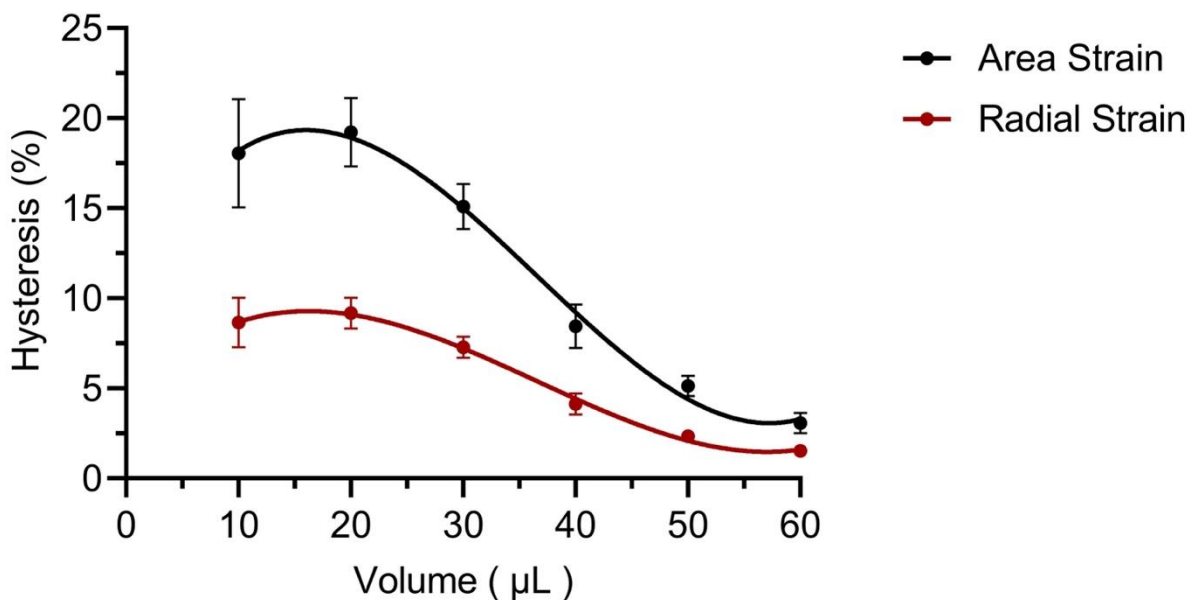


Figure S10: Plot of the strain hysteresis (%) when the different volumes of hydrogel formed. The hysteresis of the strain was calculated using the initial area of the hydrogel

and the area of the hydrogel after five strain cycles. The observed strain hysteresis was negligible compared to strain (<5%).

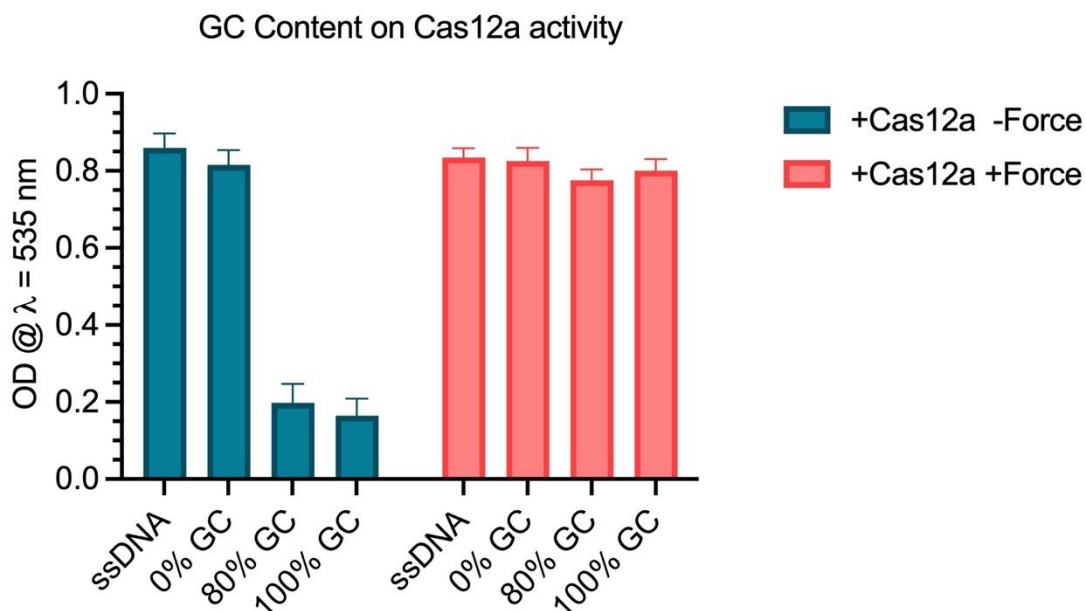


Figure S11: Bar graph indicating absorbance of released AuNPs to the buffer when the DNA crosslinked hydrogels were treated with Cas12a enzyme without external force (Blue) and with external force (orange). Both ssDNA and 0% GC DNA HP crosslinked hydrogels showed self-destruction without external force. However, 80% GC DNA HP and 100% GC DNA HP crosslinked hydrogels did not show significant degradation after 3 hours of incubation without force. Upon external force, all the hydrogels were self-destructed after 3 hours of incubation.

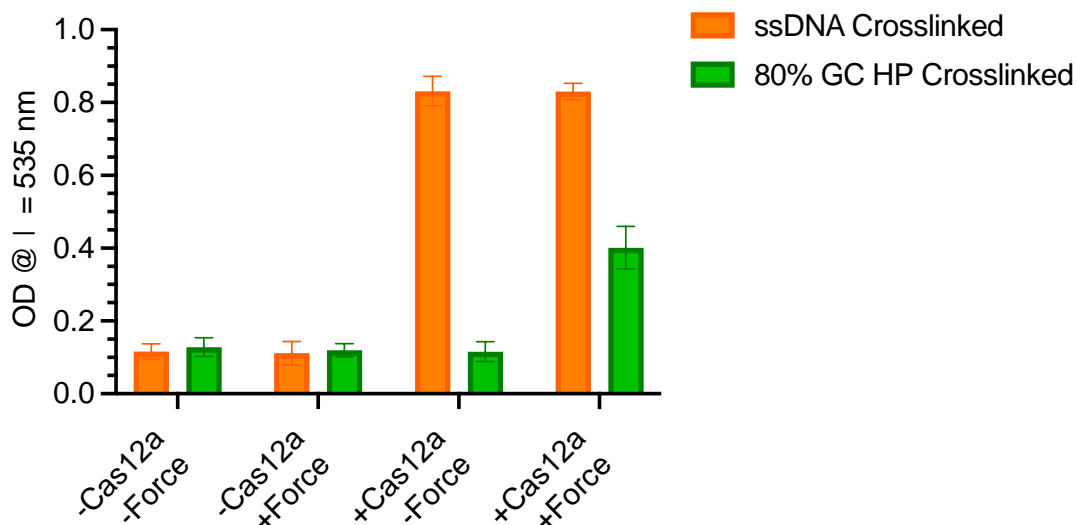


Figure S12: Bar graph indicating absorbance of released AuNPs into the buffer when the ssDNA crosslinked (orange) and 80% GC HP crosslinked (green) hydrogels were treated with/without 0.8 μM Cas12a enzyme and with/without external force (orange) after 6 hrs of incubation. Compared to higher Cas12a concentration (8.0 μM in gel) ssDNA crosslinked hydrogel did not show any difference in its self-destruction. However, DNA HP crosslinked hydrogel was partially degraded after 6 hr time point led to lower release of AuNP into the buffer.

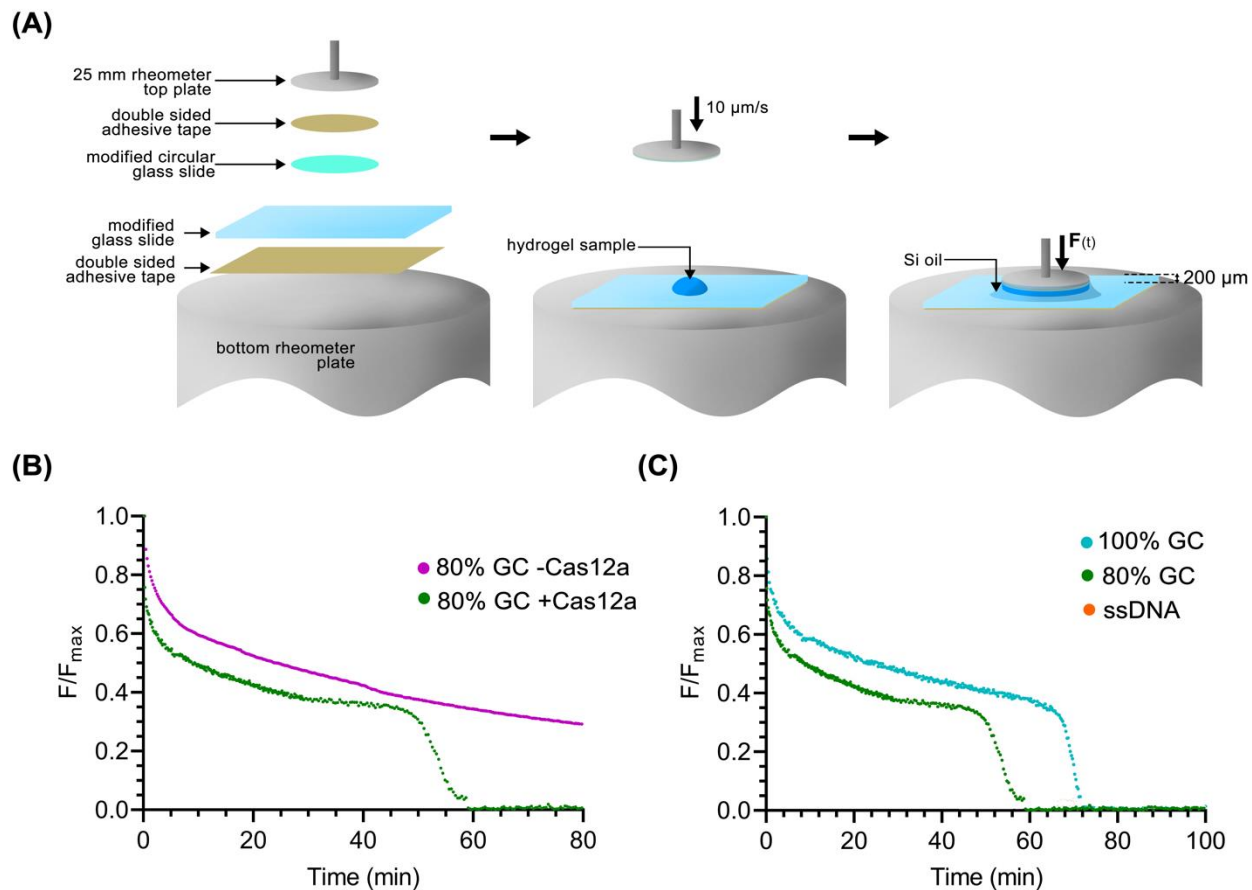


Figure S13: Characterization of the force-triggered self-destruction of the hydrogel using rheometer. **(A)** The experimental setup used to measure the force-triggered self-destruction of the hydrogel using the rheometer. **(B)** Plots of time-dependent normalized force relaxation of the DNA HP (80% GC content) crosslinked hydrogels with (green) and without (magenta) Cas12a enzyme. **(C)** Plots of time-dependent normalized force relaxation of the 80% GC content DNA HP (green), 100% GC content DNA HP (cyan), crosslinked hydrogels with Cas12a enzyme.

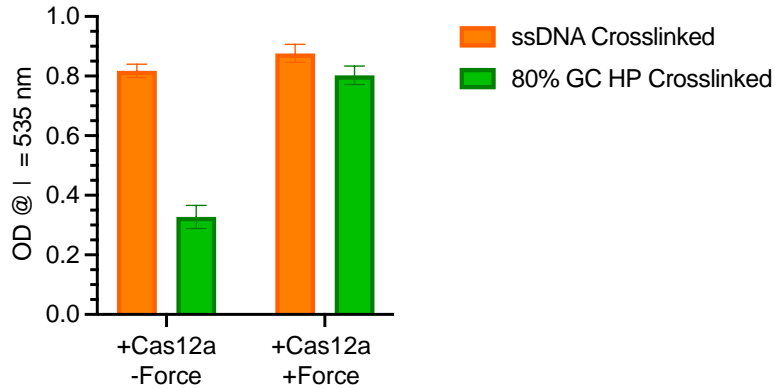


Figure S14: Bar graph indicating absorbance of released AuNPs to the buffer when the ssDNA crosslinked (orange) and 80% GC HP crosslinked (green) hydrogels were treated with/without 0.8 μ M Cas12a enzyme and with/without external force (orange) after 12 hrs of incubation at 37 $^{\circ}$ C. Importantly, Cas12a enzyme was added to the buffer after hydrogel formation in this experiment. ssDNA crosslinked hydrogel showed complete self-destruction regardless of the external force. However, DNA HP crosslinked hydrogel showed \sim 3 times less AuNP release to the buffer with the absence of the external force.

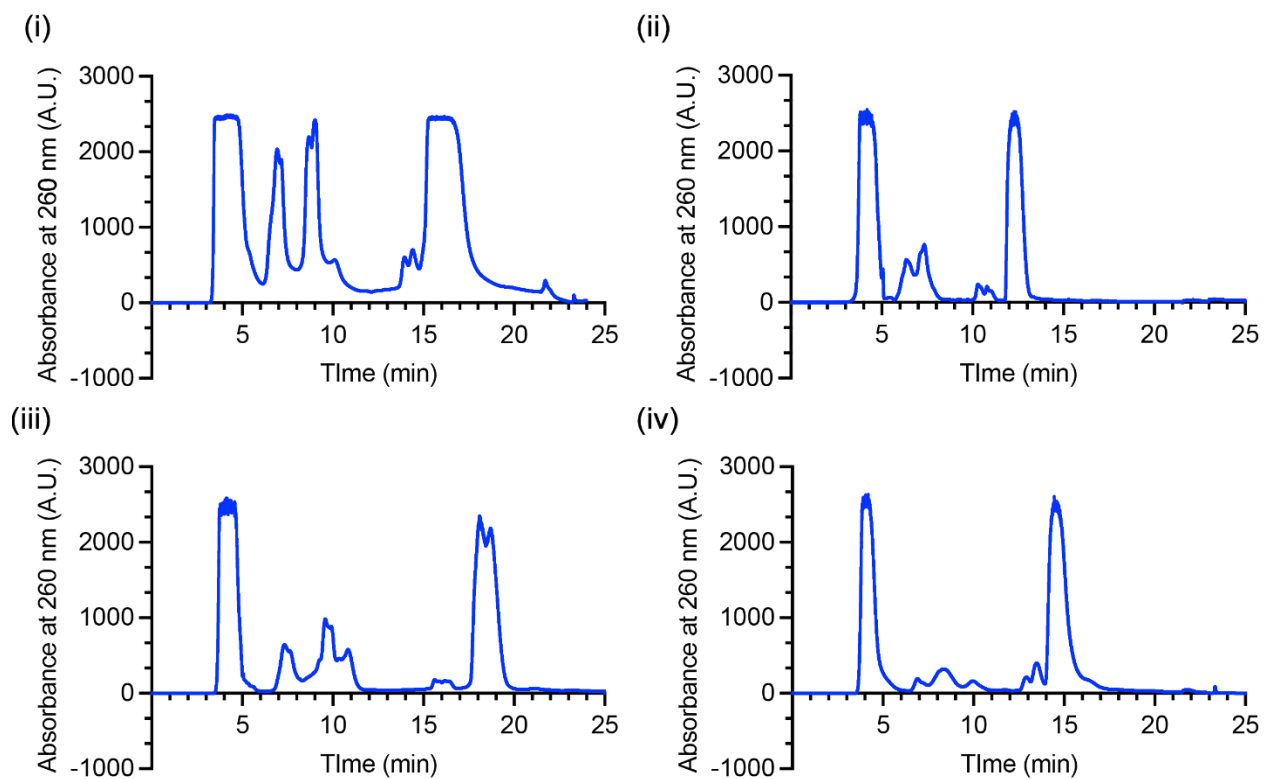
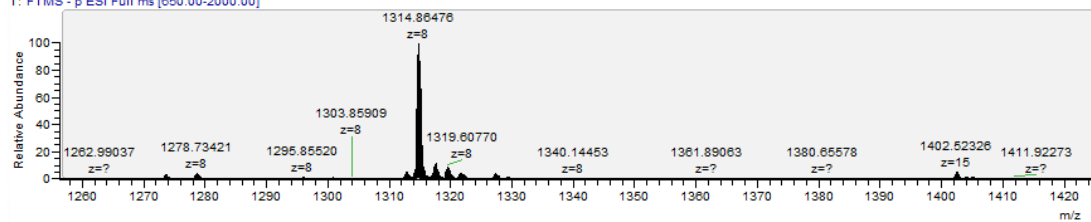


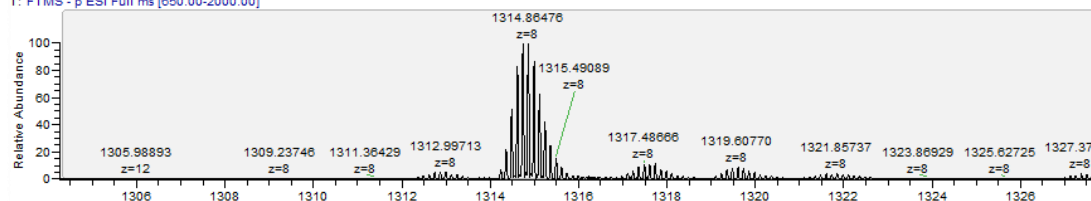
Figure S15: HPLC chromatograms of the bisazide-modified four DNA crosslinkers used in the study. **(i)** 80% GC HP (~16 min) **(ii)** ssDNA (~12.5 min) **(iii)** 100% GC HP (~18 min; note that both peaks correspond to the product) **(iv)** 0% GC HP (~15 min).

(i)

tr_wc#12-42 RT: 0.22-0.64 AV: 31 NL: 3.01E6
T: FTMS - p ESI Full ms [650.00-2000.00]

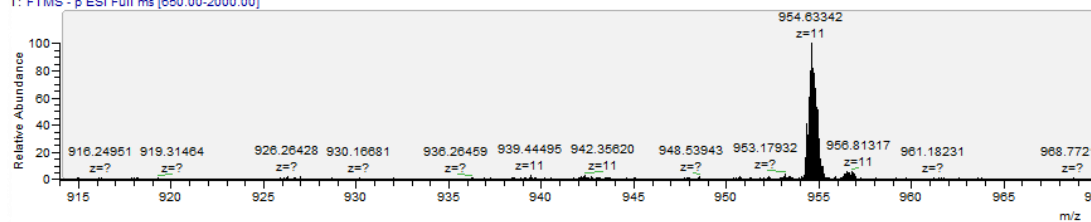


tr_wc#12-42 RT: 0.22-0.64 AV: 31 NL: 3.01E6
T: FTMS - p ESI Full ms [650.00-2000.00]

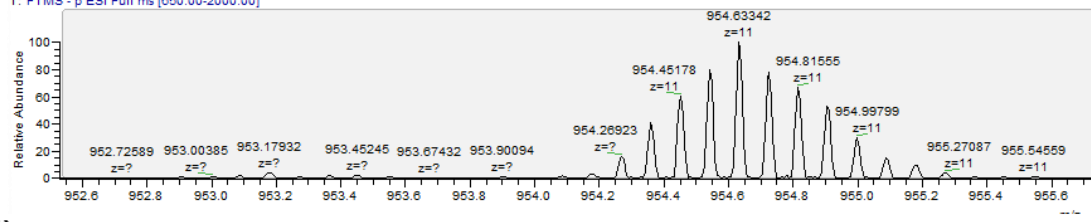


(ii)

tr_at_hp #14 RT: 0.25 AV: 1 NL: 8.84E6
T: FTMS - p ESI Full ms [650.00-2000.00]

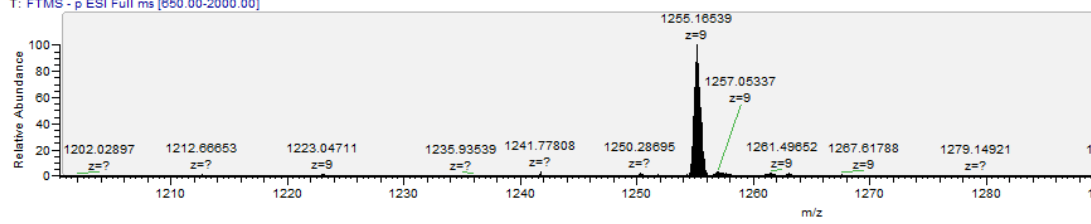


tr_at_hp #14 RT: 0.25 AV: 1 NL: 8.84E6
T: FTMS - p ESI Full ms [650.00-2000.00]



(iii)

TR_Oligo #8-22 RT: 0.10-0.29 AV: 15 NL: 2.63E6
T: FTMS - p ESI Full ms [650.00-2000.00]



TR_Oligo #8-22 RT: 0.10-0.29 AV: 15 NL: 2.63E6
T: FTMS - p ESI Full ms [650.00-2000.00]

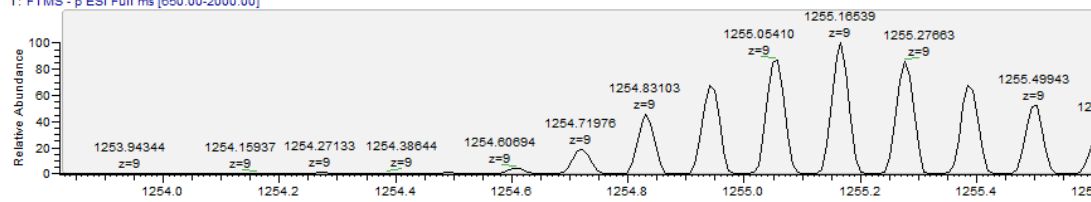


Figure S16: Observed ESI Mass spectra of the bisazide modified 100% and 0% GC DNA HP crosslinkers. **(i)** 100% GC content HP. Deconvoluted molecular weight from the spectra was $10526.9 \text{ g mol}^{-1}$. The expected molecular weight was $10527.2 \text{ g mol}^{-1}$. **(ii)** 0% GC content HP. Deconvoluted molecular weight from the spectra was $10514.1 \text{ g mol}^{-1}$. The expected molecular weight was $10512.4 \text{ g mol}^{-1}$. **(iii)** ssDNA crosslinker. Deconvoluted molecular weight from the spectra was $11305.5 \text{ g mol}^{-1}$. The expected molecular weight was $11305.6 \text{ g mol}^{-1}$.

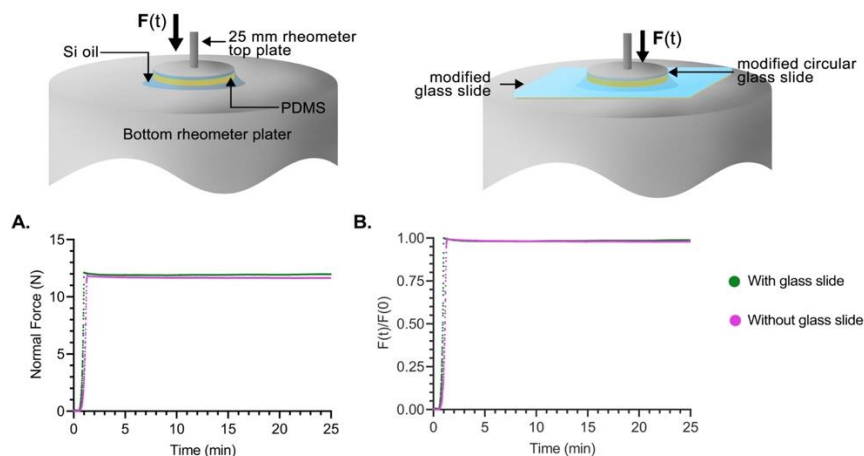


Figure S17: Plots of stress relaxation behavior of PDMS with and without glass slide. (A) Raw data for stress relaxation behavior of PDMS. (B) Normalized maximum force for stress relaxation plots. The plots shown in green are collected using the mounted glass slide, while the pink plot is for the standard metal plates. Both plots show similar relaxation profiles and maximum force of 12.10 N, and 11.94 N for plates with and without the glass slide attachment, respectively. This data shows that attaching a glass slide to the rheology metal plate does not substantially alter the stress relaxation profile when force is applied in a perpendicular orientation to the polymer.

References

[1] R. V. Gayet, H. de Puig, M. A. English, L. R. Soenksen, P. Q. Nguyen, A. S. Mao, N. M. Angenent-Mari, J. J. Collins, *Nat Protoc* 2020, 15, 3030.

[2] J. N. Zadeh, C. D. Steenberg, J. S. Bois, B. R. Wolfe, M. B. Pierce, A. R. Khan, R. M. Dirks, N. A. Pierce, *J Comput Chem* 2011, 32, 170.

[3] a)K. Barker, S. K. Rastogi, J. Dominguez, T. Cantu, W. Brittain, J. Irvin, T. Betancourt, *Journal of Biomaterials Science, Polymer Edition* 2016, 27, 22; b)M. J. Webber, E. A. Appel, B. Vinciguerra, A. B. Cortinas, L. S. Thapa, S. Jhunjhunwala, L. Isaacs, R. Langer, D. G. Anderson, *Proceedings of the National Academy of Sciences* 2016, 113, 14189.